

Radiation forces on an absorbing micrometer-sized sphere in an evanescent field

I. Brevik* and T. A. Sivertsen†

Department of Energy and Process Engineering,
Norwegian University of Science and Technology,
N-7491 Trondheim, Norway

E. Almaas‡

Department of Physics,
University of Notre Dame, Notre Dame, Indiana 46556

The vertical radiation force on an absorbing micrometer-sized dielectric sphere situated in an evanescent field is calculated, using electromagnetic wave theory. The present work is a continuation of an earlier paper [E. Almaas and I. Brevik, J. Opt. Soc. Am. B **12**, 2429 (1995)], in which both the horizontal and the vertical radiation forces were calculated with the constraint that the sphere was non-absorbing. Whereas the horizontal force can be well accounted for within this constraint, there is no possibility to describe the *repulsiveness* of the vertical force, so distinctly demonstrated in the Kawata-Sugiura experiment [Opt. Lett. **17**, 772 (1992)], unless a departure from the theory of pure non-dispersive dielectrics is made in some way. Introduction of absorption, *i.e.* a complex refractive index, is one natural way of generalizing the previous theory. We work out general expressions for the vertical force for this case and illustrate the calculations by numerical computations. It turns out that, when applied to the Kawata-Sugiura case, the repulsive radiation force caused by absorption is *not* strong enough to account for the actual lifting of the polystyrene latex or glass spheres. The physical reason for the experimental outcome is, in this case, most probably the presence of surfactants making the surface of the spheres partially conducting.

PACS numbers: 03.50.De, 42.25.-p, 42.50.Vk, 42.55.-f

I. INTRODUCTION

The outcome of the Kawata-Sugiura levitation experiment from 1992 [1] is in some ways still surprising. The authors examined the radiation force on a micrometer-sized spherical dielectric particle in the evanescent field produced by a laser beam of moderate power, $P = 150$ mW. As one would expect, the particle moved along the horizontal plate at a speed of a few micrometers per second, as a result of the tunneled photons in the evanescent field. The surprising point is, however: why does the particle *lift* from the surface? As reported in Ref. [1], “the particle is forced to float from the substrate surface and to slide along the surface.” For a non-magnetic and non-absorbing dielectric particle, it is well known that the electromagnetic volume force density \mathbf{f} is

$$\mathbf{f} = -\frac{1}{2}E^2\nabla\epsilon, \quad (1)$$

ϵ being the permittivity such that $\mathbf{f} = 0$ in the homogeneous and isotropic interior, and different from zero only in the particle’s boundary layer. The evanescent field is known to vary as $\exp[-\beta(x+h)]$ in the vertical direction (see Eq. (14) below), and is significant only very close to the substrate. In practice, this field interacts with those

parts of the particle that are situated closest to the substrate, and it gives rise to a surface force that, according to Eq. (1), has to act in the *downward* direction (assuming that $\epsilon > \epsilon_0$). It is simply impossible to account for a lift force on the particle, using Eq. (1). This discrepancy between electromagnetic theory for dielectrics and the Kawata-Sugiura experiment [1] is therefore, as mentioned above, somewhat surprising at first sight, since Eq. (1) has generally been proven to be invaluable in a multitude of cases in electromagnetism and optics.

Consequently, we have to conclude that the explanation for the observed lift of the particle has to lie in the presence of an additional force, different from the one given by Eq. (1). The following two possibilities come to mind:

(1) The particle has a complex permittivity ϵ , and is therefore exposed to a repulsive (or positive lift) force caused by the absorption of radiation in the interior.

(2) Another natural possibility is that *surface effects* may have played a significant role in the experiments. The presence of impurities on the surface, or the presence of a liquid or a film of adsorbed material, may have a considerable influence on the electrical conductivity of the surface region, and can thus enhance multiple scattering effects. This allows for an analysis of the problem in terms of a multiple scattering formalism. Adopting such a picture, the vertical force on the particle necessarily has to be repulsive; the photons are bouncing off the spherical surface and are, accordingly, transferring an impulse in the upward direction.

In the present paper, we will be studying option (1)

*Electronic address: iver.h.brevik@mtf.ntnu.no

†Electronic address: Tom-Arne.Sivertsen@ffi.no

‡Electronic address: Almaas.1@nd.edu

above, thus allowing for a complex ϵ , which in turn implies a non-vanishing effective conductivity σ in the interior of the particle. As far as we know, such a study has not previously been undertaken. This study is a continuation of the work of Almaas and Brevik [2], dealing with the case of a pure dielectric (real ϵ). Whereas the analysis in [2] gave satisfactory results for the *horizontal* radiation force observed in the Kawata-Sugiura experiment, it was impossible, as mentioned above, on the basis of Eq. (1) to account for an upward directed vertical force. From now on, we will assume that the particle is a sphere of radius a , and regard the effective conductivity σ as an input parameter.

Before embarking on the mathematical formalism, let us however make some further remarks related to option (2) above. There is a variety of surface effects that one can envisage: multiple reflections, as mentioned; moreover capillary forces (the order of magnitude of the capillary forces may be up to 10^{-7} N), surface tension (because of the capillary forces), viscous retarding forces if the sphere and the surface are immersed in a liquid, electrostatic forces, and finally the role of evaporation. Cf. in this context the survey given by Vilfan *et al.* [3]. Especially the role of the *size* of the spherical particle seems to be important. If the particle is large, multiple scattering between the sphere and the substrate distorts the evanescent wave structure that one would have in the absence of the particle. Lester and Nieto-Vesperinas [4] recently analyzed the problem using multiple scattering methods, and were able to account for a positive lift force. An advantage of this kind of method is that the proximity of the sphere-substrate two-body system is addressed explicitly. In contrast, our formalism is built on the model of scattering of an evanescent wave by an isolated sphere, and is therefore not expected to be very accurate for small separations between the sphere and the substrate. It is necessary to point out that the adoption of a multiple scattering method does not *in itself* imply that the lift force is positive, as long as the material in the sphere is a pure dielectric. Regardless of whether the electromagnetic boundary conditions at the surface of the substrate are taken into account or not, for a pure dielectric, the force on the sphere is given by Eq. (1), and, as we have argued above, is necessarily downward directed. To account for a positive lift force, we must allow for deviations from the simple theory of pure dielectrics, meaning that absorption, and consequently conductivity, are important effects in the theory, explicitly or implicitly.

As already mentioned, we will not attempt to give a quantitative description of a possible adsorbed film on the surface; the physical reason for such a film may be quite complex. Problems of this sort belong to the vast field of physicochemical hydrodynamics. [A good source of information in this area is the book of Levich [5]; a briefer treatment is found in Landau and Lifshitz [6]]. It is noticeable that the experiment of Vilfan *et al.* [3] similarly measured a repulsive force. They obtained a force 300 pN on a dielectric sphere of radius $5 \mu\text{m}$ in the

evanescent field of a 500 mW laser focused to a diameter of $5 \mu\text{m}$. These spheres are relatively large, and are therefore likely to distort the evanescent field structure considerably.

In the next section, we summarize the wave theoretical formalism describing the interaction between the evanescent field and the sphere. In Section 3, we show how the surface force \mathbf{F}^{surf} – *i.e.* the part of the total radiation force \mathbf{F} which is associated with the boundary and independent of the absorptive properties in the interior – can be written as a double sum over complex expansion coefficients. Section 4, the main section of our paper, contains the calculation of the absorptive part \mathbf{F}^{abs} of the radiation force. The results are illustrated in Figs. 2 - 5. Our calculations incorporate both the two polarization states of the incident beam (p and s polarization).

Our main analytical result is given in Eq. (66), for the non-dimensional vertical absorptive force component Q_x^{abs} . As one would expect physically, the result becomes proportional to the effective conductivity σ . For the polystyrene latex spheres, or glass spheres, used in the Kawata-Sugiura experiment, the values of σ are low. Hence, it turns out that Q_x^{abs} becomes too weak to account for the floating of the sphere in the gravitational field. Now, our formalism has, of course, a much wider scope than the Kawata-Sugiura experiment. In optics, there are numerous cases where radiation forces interact with absorbing media. For instance, the current development of microelectromagnetical systems, which are used in a variety of applications including even measurements of the Casimir force, accentuates the usefulness of the present theory.

II. BASIC FORMALISM

A sketch of the geometry is shown in Fig. 1: A laser beam is incident from below through a transparent medium, called medium 1, and hits the plane, horizontal surface towards the transparent medium 2 at an angle of incidence, θ_1 , which is greater than the critical angle, $\theta_{\text{crit}} = \arcsin(n_2/n_1)$, for total reflection. This establishes an evanescent field above the plane surface, which, in turn, is regarded as the incident field falling upon a compact sphere of radius a and complex refractive index \bar{n}_3 . The sphere is centered at the origin with the x axis pointing vertically upwards. If $\bar{\epsilon}_3$ is the complex permittivity of the (non-magnetic) sphere, we will require it to be related to the effective conductivity, σ , through the equation

$$\bar{\epsilon}_3 = \epsilon_3 + i\sigma/\omega, \quad (2)$$

hence $\bar{n}_3 = \sqrt{\bar{\epsilon}_3/\epsilon_0}$.

Here, a remark is called for as regards our formal use of the dispersion relation. For simplicity, taking the medium to have only one resonance frequency, we can

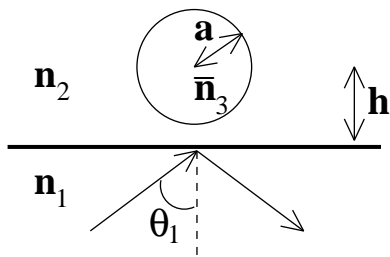


FIG. 1: Spherical particle of radius a , with complex refractive index \bar{n}_3 , situated in an evanescent field with its center at a height h above the plane substrate. A laser beam is incident from below at an angle of incidence $\theta_1 > \theta_{crit}$. Refractive indices in the transparent media 1 and 2 are respectively n_1 and n_2 .

write the complex permittivity as

$$\bar{\epsilon}(\omega) = \epsilon_3 + i \frac{\epsilon_0 \omega_p^2}{\omega(\gamma - i\omega)}; \quad (3)$$

cf., for instance, Eq. (7.56) in Jackson [7]. Here the first term ϵ_3 describes the contribution from the dipoles and can be taken to be constant, whereas the second term describes the dispersive properties of the free electrons. γ is the damping constant. Comparison between Eqs. (2) and (3) gives for the frequency dependent term $\sigma(\omega)$

$$\sigma(\omega) = \frac{\epsilon_0 \omega_p^2}{\gamma - i\omega}. \quad (4)$$

Typically $\gamma \sim 10^{12} \text{ s}^{-1}$, so that we can identify the frequency dependent quantity $\sigma = \sigma(\omega)$ with a constant, equal to the static conductivity σ_{stat} , only for frequencies $\nu = \omega/2\pi$ less than about 10 GHz. Our frequencies are obviously higher: a vacuum wavelength of $\lambda_0 = 1.06 \mu\text{m}$ corresponds to $\omega_0 = 1.78 \times 10^{15} \text{ s}^{-1}$. Thus our $\sigma(\omega)$ is an *effective* conductivity, defined in accordance with the low-frequency relation (2), but no longer identifiable with the static conductivity σ_{stat} . The actual value of $\sigma(\omega)$ has to be evaluated in each case.

Take water as an example, for which $\bar{n} = 1.33 + 5.0 \times 10^{-6}i$ for the actual wavelength [8]. Writing in general the complex refractive index as $\bar{n} = n' + in''$ we get, when $\sigma/\epsilon_0\omega \ll 1$, $\sigma/\epsilon_0\omega = 2n'n''$, which in our case amounts to only 1.33×10^{-5} , corresponding to

$$\sigma = 0.21 \text{ S/m}. \quad (5)$$

This can be compared with the static conductivity for pure water, which is much smaller, $\sigma_{stat} = 2 \times 10^{-4} \text{ S/m}$ [9]. It is notable that the value of σ is real.

Increasing the incident wavelength somewhat, the absorptive effect can be enhanced. Thus, if we consider glass, and choose $\lambda_0 = 8.0 \mu\text{m}$, we have $\bar{n} = 0.411 + 0.323i$ [10]. With $\omega = 2.36 \times 10^{14} \text{ s}^{-1}$ in this case we get for the effective conductivity quite an appreciable value:

$$\sigma = 550 \text{ S/m}. \quad (6)$$

(Actually the parameter $\sigma/\epsilon_0\omega$ is as high as 0.265 in this case, and can hardly be assumed to be a "small" parameter any longer if λ_0 is increased further.)

We assume now that the incoming beam in medium 1 is a plane wave, such that its electric and magnetic field amplitudes are related through $H_0 = \sqrt{\epsilon_0/\mu_0} E_0$. We introduce the non-dimensional wave number, α , in medium 2, and the relative radial coordinate \tilde{r} :

$$\alpha = k_2 a = n_2 \omega a / c, \quad \tilde{r} = r/a, \quad (7)$$

and make use of the standard spherical coordinates (r, θ, φ) centered at the origin of the sphere. Expansions for the incident electric field $\mathbf{E}^{(i)} = (E_r^{(i)}, E_\theta^{(i)}, E_\varphi^{(i)})$, the scattered field $\mathbf{E}^{(s)} = (E_r^{(s)}, E_\theta^{(s)}, E_\varphi^{(s)})$, and the internal field in the sphere, $\mathbf{E}^{(w)} = (E_r^{(w)}, E_\theta^{(w)}, E_\varphi^{(w)})$, are for convenience collected in Appendix A together with the analogous expansions of the magnetic field. In these expressions, we have imposed the electromagnetic boundary conditions at the spherical surface, $r = a$. We will need use of the Riccati-Bessel functions ψ_l and $\xi_l^{(1)}$:

$$\psi_l(x) = x j_l(x), \quad \xi_l^{(1)}(x) = x h_l^{(1)}(x). \quad (8)$$

Here, j_l and h_l are the spherical Bessel and Hankel functions, satisfying the Wronskian $W\{\psi_l, \xi_l^{(1)}\} = i$. There are three groups of expansion coefficients: $\{A_{lm}, B_{lm}\}$ for the incident field, $\{a_{lm}, b_{lm}\}$ for the scattered field, and $\{c_{lm}, d_{lm}\}$ for the internal field. As for the first-mentioned coefficients, they are determined by inverting the formulas (A.1) and (A.4) for $E_r^{(i)}$ and $H_r^{(i)}$:

$$A_{lm} = \frac{(b/a)^2}{E_0 l(l+1) \psi_l(k_2 b)} \int_{\Omega} E_r^{(i)}(b, \theta, \varphi) Y_{lm}^*(\theta, \varphi) d\Omega, \quad (9)$$

$$B_{lm} = \frac{(b/a)^2}{H_0 l(l+1) \psi_l(k_2 b)} \int_{\Omega} H_r^{(i)}(b, \theta, \varphi) Y_{lm}^*(\theta, \varphi) d\Omega, \quad (10)$$

where $d\Omega = \sin \theta d\theta d\varphi$. Here, the angular integrations are taken over a sphere of arbitrary radius b . This freedom of choice for b gives us a calculational advantage. The results for A_{lm} and B_{lm} are only related to the incident field, and they have to be independent of b . Calculational insensitivity with respect to various input values for b thus serves as a check of the evaluations of A_{lm} and B_{lm} . In the following, we will suppress the writing of the time factors $\exp(-i\omega t)$.

Our expansion procedure follows the conventions of Barton *et al.* [8, 11]. This procedure was also followed in Ref. [2]. In the case where b is chosen equal to a , Eqs. (9) and (10) agree with Eqs. (A.23) and (A.24) of Ref. [11].

In order to calculate A_{lm} and B_{lm} , it is necessary to know the incident field components $E_r^{(i)} \equiv E_r^{(2)}$ and $H_r^{(i)} \equiv H_r^{(2)}$ in region 2. We introduce the parameters

$$\beta = \frac{n_1 \omega}{c} \sqrt{\sin^2 \theta_1 - n_{21}^2}, \quad \gamma = \frac{n_1 \omega}{c} \sin \theta_1, \quad n_{21} = \frac{n_2}{n_1}, \quad (11)$$

and take the following expressions for the amplitude ratios, $T_{\parallel} = E_{\parallel}^{(2)}/E_{\parallel}^{(1)}$, and $T_{\perp} = E_{\perp}^{(2)}/E_{\perp}^{(1)}$ at the surface of the substrate into account:

$$T_{\parallel} = \frac{2n_{21} \cos \theta_1}{n_{21}^2 \cos \theta_1 + i\sqrt{\sin^2 \theta_1 - n_{21}^2}}, \quad (12)$$

$$T_{\perp} = \frac{2 \cos \theta_1}{\cos \theta_1 + i\sqrt{\sin^2 \theta_1 - n_{21}^2}}. \quad (13)$$

Here, E_{\parallel} refers to the field component in the plane of incidence (p polarization), and E_{\perp} to the field orthogonal to it (s polarization). For the radial field components, we find

$$E_r^{(i)} = \left\{ \frac{1}{n_{21}} T_{\parallel} E_{\parallel}^{(1)} [\sin \theta_1 \sin \theta \cos \varphi - i\sqrt{\sin^2 \theta_1 - n_{21}^2} \cos \theta] + T_{\perp} E_{\perp}^{(1)} \sin \theta \sin \varphi \right\} \times \exp[-\beta(x+h) + i\gamma z], \quad (14)$$

$$H_r^{(i)} = \left\{ T_{\perp} H_{\parallel}^{(1)} [-\sin \theta_1 \sin \theta \cos \varphi + i\sqrt{\sin^2 \theta_1 - n_{21}^2} \cos \theta] + n_{21} T_{\parallel} H_{\perp}^{(1)} \sin \theta \sin \varphi \right\} \times \exp[-\beta(x+h) + i\gamma z], \quad (15)$$

where

$$H_{\parallel}^{(2)}/H_{\parallel}^{(1)} = n_{21} T_{\perp}, \quad H_{\perp}^{(2)}/H_{\perp}^{(1)} = n_{21} T_{\parallel}, \quad (16)$$

at the surface of the substrate. (Readers interested in background material for our developments can *e.g.* consult the articles [2, 8, 11, 12], as well as the standard texts [9, 13, 14].) Upon insertion into Eqs. (9) and (10), we find that the coefficients A_{lm} and B_{lm} for the case of s (\perp) and p (\parallel) polarization are related through

$$A_{lm}^{\perp} = \frac{T_{\perp}}{n_2 T_{\parallel}} B_{lm}^{\parallel}, \quad (17)$$

$$B_{lm}^{\perp} = -\frac{n_2 T_{\perp}}{T_{\parallel}} A_{lm}^{\parallel}, \quad (18)$$

hence, it is sufficient to only consider one polarization direction in the calculations of the expansion coefficients, and in the following, we will choose the case of p polarization. By inserting the expressions for the incident field into Eqs. (9) and (10), we obtain the following expressions for the expansion coefficients:

$$A_{lm}^{\parallel} = \frac{\alpha_1(l, m)}{n_{21}} T_{\parallel} e^{-\beta h} \left[\sin \theta_1 Q_1(l, m) - i\sqrt{\sin^2 \theta_1 - n_{21}^2} Q_2(l, m) \right], \quad (19)$$

$$B_{lm}^{\parallel} = n_2 \alpha_1(l, m) T_{\parallel} e^{-\beta h} Q_3(l, m), \quad (20)$$

where we have defined

$$\alpha_1(l, m) = \left[\frac{2l+1}{4\pi} \frac{(l-m)!}{(l+m)!} \right]^{1/2} \frac{(b/a)^2}{l(l+1)\psi_l(k_2 b)}, \quad (21)$$

$$Q_1(l, m) = 2\pi(-1)^{m-1} \int_0^{\pi/2} \sin^2 \theta \left\{ \begin{array}{c} \cos \\ i \sin \end{array} \right\} (\gamma b \cos \theta) \times P_l^m(\cos \theta) [I_{|m-1|}(u) + I_{|m+1|}(u)] d\theta, \quad (22)$$

$$Q_2(l, m) = 4\pi(-1)^m \int_0^{\pi/2} \sin \theta \cos \theta \left\{ \begin{array}{c} i \sin \\ \cos \end{array} \right\} (\gamma b \cos \theta) \times P_l^m(\cos \theta) I_{|m|}(u) d\theta, \quad (23)$$

$$Q_3(l, m) = 4\pi i(-1)^m \frac{m}{\beta b} \int_0^{\pi/2} \sin \theta \left\{ \begin{array}{c} \cos \\ i \sin \end{array} \right\} (\gamma b \cos \theta) \times P_l^m(\cos \theta) I_{|m|}(u) d\theta, \quad (24)$$

where $u = \beta b \sin \theta$, $l+m$ is $\left\{ \begin{array}{c} \text{even} \\ \text{odd} \end{array} \right\}$, and $I_m(z) = i^{-m} J_m(iz)$ is a modified Bessel function. (In Ref. [2], Eqs. (46) and (49), were missing factors of 2.) Again, the calculated values of A_{lm}^{\parallel} and B_{lm}^{\parallel} have to be numerically independent of the value chosen for the radius b .

Once A_{lm} and B_{lm} are known, the other sets of coefficients, $\{a_{lm}, b_{lm}\}$ and $\{c_{lm}, d_{lm}\}$, can readily be calculated using Eqs. (A.19)–(A.22). In appendix B, we give a table of A_{lm} and B_{lm} up to $l_{\max} = 7$ for p polarization.

III. THE SURFACE FORCE

Let us, as indicated above, write the total radiation force \mathbf{F} on the sphere as a sum of two contributions:

$$\mathbf{F} = \mathbf{F}^{\text{surf}} + \mathbf{F}^{\text{abs}}, \quad (25)$$

where \mathbf{F}^{surf} is the result of the force density \mathbf{f} acting in the surface layer, *i.e.* Eq. (1), and \mathbf{F}^{abs} is caused by the absorption in the sphere. By integrating across the surface layer, the components F_i^{surf} of \mathbf{F}^{surf} can be related to the surface integral of Maxwell's stress tensor S_{ik} on the outside of the sphere:

$$F_i^{\text{surf}} = - \int S_{ik} n_k dS, \quad (26)$$

\mathbf{n} being the outward normal (cf. for instance, Refs. [11, 15]). [This expression assumes that the effect from

absorption is negligible, in other words that the size of the particle is much smaller than the skin depth $\delta = (2/\mu_0\omega\sigma)^{1/2}$.] If $a \ll \lambda_0$, and the susceptibility of the particle is small, the formula for the total force \mathbf{F} goes over to the conventional expression for dilute particles:

$$\mathbf{F} = 6\pi a^3 \frac{\epsilon''}{(\epsilon + 2\epsilon_0)^2} \epsilon_0 \mathbf{k} |E^{(i)}|^2; \quad (27)$$

cf., for instance, Refs. [16, 17, 18].

It should be stressed that we are calculating the force

on the sphere in two steps: First, the surface integral (26) is evaluated assuming the refractive index to be real. That means, the coefficients A_{lm} and B_{lm} below are calculated on the basis of a real n_3 . Thereafter, the absorptive part \mathbf{F}^{abs} is calculated separately, via the force density $\mathbf{J} \times \mathbf{B}$.

Using the general expressions for the incident and the scattered field, Eqs. (A.1) – (A.12), we can re-write this surface integral in terms of the complex expansion coefficients A_{lm} , B_{lm} , a_{lm} and b_{lm} :

$$\begin{aligned} \frac{F_x^{\text{surf}} + iF_y^{\text{surf}}}{\epsilon_0 E_0^2 a^2} &= \frac{i\alpha^2}{4} \sum_{l=1}^{\infty} \sum_{m=-l}^l \left\{ \left[\frac{(l+m+2)(l+m+1)}{(2l+1)(2l+3)} \right]^{1/2} l(l+2) \left(2n_2^2 a_{lm} a_{l+1,m+1}^* + n_2^2 a_{lm} A_{l+1,m+1}^* \right. \right. \\ &+ n_2^2 A_{lm} a_{l+1,m+1}^* + 2b_{lm} b_{l+1,m+1}^* + b_{lm} B_{l+1,m+1}^* + B_{lm} b_{l+1,m+1}^* \left. \right) + \left[\frac{(l-m+1)(l-m+2)}{(2l+1)(2l+3)} \right]^{1/2} \\ &\times l(l+2) \left(2n_2^2 a_{l+1,m-1} a_{lm}^* + n_2^2 a_{l+1,m-1} A_{lm}^* + n_2^2 A_{l+1,m-1} a_{lm}^* + 2b_{l+1,m-1} b_{lm}^* + b_{l+1,m-1} B_{lm}^* \right. \\ &+ B_{l+1,m-1} b_{lm}^* \left. \right) - \left[(l+m+1)(l-m) \right]^{1/2} n_2 \left(-2a_{lm} b_{l,m+1}^* + 2b_{lm} a_{l,m+1}^* - a_{lm} B_{l,m+1}^* \right. \\ &\left. \left. + b_{lm} A_{l,m+1}^* + B_{lm} a_{l,m+1}^* - A_{lm} b_{l,m+1}^* \right) \right\}, \quad (28) \end{aligned}$$

$$\begin{aligned} \frac{F_z^{\text{surf}}}{\epsilon_0 E_0^2 a^2} &= -\frac{\alpha^2}{2} \sum_{l=1}^{\infty} \sum_{m=-l}^l \left[\frac{(l-m+1)(l+m+1)}{(2l+1)(2l+3)} \right]^{1/2} l(l+2) \Im \left[2n_2^2 a_{l+1,m} a_{lm}^* + n_2^2 a_{l+1,m} A_{lm}^* + n_2^2 A_{l+1,m} a_{lm}^* \right. \\ &\left. + 2b_{l+1,m} b_{lm}^* + b_{l+1,m} B_{lm}^* + B_{l+1,m} b_{lm}^* + n_2 m (2a_{lm} b_{lm}^* + a_{lm} B_{lm}^* + A_{lm} b_{lm}^*) \right]. \quad (29) \end{aligned}$$

We shall not dwell much on these expressions, since our main interest, as mentioned above, is the vertical force F_x^{abs} associated with the absorption. Consider, however, the horizontal surface force component F_z^{surf} . With an incident beam power (in vacuum) of $P = 150$ mW, distributed over a circular cross-sectional area of diameter $10 \mu\text{m}$, we find the magnitude of the Poynting vector to be $(c/2)\epsilon_0 E_0^2 = 19.0 \text{ MW}/\text{m}^2$. Taking the radius of the sphere $a = 1 \mu\text{m}$, we find the denominator in Eq. (29) to be $\epsilon_0 E_0^2 a^2 = 0.13 \text{ pN}$. If the sphere is made of glass ($n_3 = 1.50$) and the surrounding medium 2 is water ($n_2 = 1.33$), we then have $\alpha = 2\pi a/\lambda_2 = 7.9$, since the wavelength in water for Nd:YAG laser light is $\lambda_2 = 1.06/1.33 = 0.80 \mu\text{m}$. Using Fig. 5 in Ref. [2], we find that F_z^{surf} is positive, as it should be, and is approximately equal to 0.010 pN in the case of p polarization. Since the Reynolds number is very low, the Stokes drag formula $D = 6\pi\mu a v$ is applicable, using $\mu = 1.0 \times 10^{-3} \text{ Pa s}$ as the dynamic viscosity of water. Putting $F_z^{\text{surf}} = D$, we obtain the drift velocity of the sphere to be $v = 0.53 \mu\text{m/s}$. This is an order of magnitude agreement with the

observations of Kawata and Sugiura [1]; from their Fig. 4, one infers that $v \sim 1 - 2 \mu\text{m/s}$. This agreement is satisfactory; there is no need to carry out a complicated calculation to find the absorptive correction to the horizontal radiation force. In the following, we focus attention on the vertical absorptive part of the force.

IV. THE VERTICAL ABSORPTIVE FORCE

To calculate the absorptive force, we first replace Eq. (1) by the general expression

$$\mathbf{f} = \rho \mathbf{E} + \mathbf{J} \times \mathbf{B} - \frac{1}{2} E^2 \nabla \epsilon, \quad (30)$$

where ρ and \mathbf{J} are the external charge and current densities in the medium. A general derivation of this force expression can be found, for instance, in Stratton's book [9]. Also, in the review article of one of the present authors [15], it was found that the force expression is able to

describe the outcome of known experiments. We assume no external charges to be present, so that $\rho = 0$. Writing $\mathbf{J} = \sigma \mathbf{E}$ where σ is the frequency-dependent conductivity, assumed to be real (cf. Eq. (5)), we get in complex representation the following expression for the absorptive force:

$$\mathbf{F}^{\text{abs}} = \frac{1}{2} \Re \int \mathbf{J} \times \mathbf{B}^* dV = \frac{\sigma \mu_0}{2} \Re \int \mathbf{E} \times \mathbf{H}^* dV, \quad (31)$$

where the integral is evaluated over the volume of the sphere.

In cases of current interest, we can simplify our calculation: In view of the assumed smallness of $\sigma/\epsilon_0\omega$, we replace the fields inside the sphere with those calculated when assuming the material to be a perfect dielectric. That is, we can replace the complex refractive index \bar{n}_3 by its real part n_3 . This facilitates the calculation of the volume integrals. The expressions for the internal fields are given by Eqs. (A.13)–(A.18), in spherical coordinates. For notational convenience, we will omit the superscripts (w).

With $\tilde{r} = r/a$ we can write the vertical absorptive force as

$$\begin{aligned} F_x^{\text{abs}} &= \frac{\sigma \mu_0}{2} a^3 \Re \int_0^{2\pi} d\varphi \int_0^\pi \sin \theta d\theta \int_0^1 \tilde{r}^2 d\tilde{r} \left[(\mathbf{E} \times \mathbf{H}^*)_r \right. \\ &\quad \left. \times \sin \theta \cos \varphi + (\mathbf{E} \times \mathbf{H}^*)_\theta \cos \theta \cos \varphi - (\mathbf{E} \times \mathbf{H}^*)_\varphi \sin \varphi \right], \\ &= \frac{\sigma \mu_0}{2} a^3 \Re \sum_{i=1}^6 I_i, \end{aligned} \quad (32)$$

where we have defined

$$I_1 = \int_0^{2\pi} \cos \varphi d\varphi \int_0^\pi \sin^2 \theta d\theta \int_0^1 \tilde{r}^2 d\tilde{r} E_\theta H_\varphi^*, \quad (33)$$

$$I_2 = - \int_0^{2\pi} \cos \varphi d\varphi \int_0^\pi \sin^2 \theta d\theta \int_0^1 \tilde{r}^2 d\tilde{r} E_\varphi H_\theta^*, \quad (34)$$

$$I_3 = \int_0^{2\pi} \cos \varphi d\varphi \int_0^\pi \cos \theta \sin \theta d\theta \int_0^1 \tilde{r}^2 d\tilde{r} E_\varphi H_r^*, \quad (35)$$

$$I_4 = - \int_0^{2\pi} \cos \varphi d\varphi \int_0^\pi \cos \theta \sin \theta d\theta \int_0^1 \tilde{r}^2 d\tilde{r} E_r H_\varphi^*, \quad (36)$$

$$I_5 = - \int_0^{2\pi} \sin \varphi d\varphi \int_0^\pi \sin \theta d\theta \int_0^1 \tilde{r}^2 d\tilde{r} E_r H_\theta^*, \quad (37)$$

$$I_6 = \int_0^{2\pi} \sin \varphi d\varphi \int_0^\pi \sin \theta d\theta \int_0^1 \tilde{r}^2 d\tilde{r} E_\theta H_r^*. \quad (38)$$

It is now convenient to introduce the operators

$$\mathcal{L} = \sum_{l=1}^{\infty} \sum_{j=1}^{\infty} \int_0^{n_{32} \alpha} du, \quad (39)$$

$$\mathcal{M}_{lj}^{(\pm)} = \sum_{m=-l}^l \sum_{k=-j}^j (\delta_{m,k-1} \pm \delta_{m,k+1}). \quad (40)$$

We write the two first of the I_i 's as a sum of four terms:

$$I_i = i\pi \alpha n_1 c \epsilon_0 E_0^2 \sum_{k=1}^4 I_{ik}, \quad i = 1, 2. \quad (41)$$

and remaining I_i 's, which are simpler since they are each composed of only two terms:

$$I_i = i\pi \alpha n_1 c \epsilon_0 E_0^2 \sum_{k=1}^2 I_{ik}, \quad i = 3, 4, 5, 6. \quad (42)$$

where (in the following, l , m , j and k denote summation indices as defined in Eqs. (39) and (40))

$$I_{11} = -n_{32} \mathcal{L} \left[\psi'_l(u) \psi'_j(u) \mathcal{M}_{lj}^{(+)} \left\{ k c_{lm} d_{jk}^* C_{lm} C_{jk} \mathcal{R}_1(l, m, j, k) \right\} \right], \quad (43)$$

$$I_{12} = -n_{32}^2 n_2 \mathcal{L} \left[\psi'_l(u) \psi_j(u) \mathcal{M}_{lj}^{(+)} \left\{ c_{lm} c_{jk}^* C_{lm} C_{jk} \mathcal{R}_2(l, m, j, k) \right\} \right], \quad (44)$$

$$I_{13} = \frac{1}{n_2} \mathcal{L} \left[\psi_l(u) \psi'_j(u) \mathcal{M}_{lj}^{(+)} \left\{ m k d_{lm} d_{jk}^* C_{lm} C_{jk} \mathcal{R}_3(l, m, j, k) \right\} \right], \quad (45)$$

$$I_{14} = n_{32} \mathcal{L} \left[\psi_l(u) \psi_j(u) \mathcal{M}_{lj}^{(+)} \left\{ m d_{lm} c_{jk}^* C_{lm} C_{jk} \mathcal{R}_1(j, k, l, m) \right\} \right], \quad (46)$$

$$I_{21} = -n_{32} \mathcal{L} \left[\psi'_l(u) \psi'_j(u) \mathcal{M}_{lj}^{(+)} \left\{ m c_{lm} d_{jk}^* C_{lm} C_{jk} \mathcal{R}_1(j, k, l, m) \right\} \right], \quad (47)$$

$$I_{22} = -n_{32}^2 \mathcal{L} \left[\psi'_l(u) \psi_j(u) \mathcal{M}_{lj}^{(+)} \left\{ m k c_{lm} c_{jk}^* C_{lm} C_{jk} \mathcal{R}_3(l, m, j, k) \right\} \right], \quad (48)$$

$$I_{23} = \frac{1}{n_2} \mathcal{L} \left[\psi_l(u) \psi'_j(u) \mathcal{M}_{lj}^{(+)} \left\{ d_{lm} d_{jk}^* C_{lm} C_{jk} \mathcal{R}_2(l, m, j, k) \right\} \right], \quad (49)$$

$$I_{24} = n_{32} \mathcal{L} \left[\psi_l(u) \psi_j(u) \mathcal{M}_{lj}^{(+)} \left\{ k d_{lm} c_{jk}^* C_{lm} C_{jk} \mathcal{R}_1(l, m, j, k) \right\} \right], \quad (50)$$

$$I_{31} = n_{32} \mathcal{L} \left[\frac{\psi'_l(u)}{u} \psi_j(u) j(j+1) \mathcal{M}_{lj}^{(+)} \left\{ m c_{lm} d_{jk}^* C_{lm} C_{jk} \mathcal{R}_4(l, m, j, k) \right\} \right], \quad (51)$$

$$I_{32} = -\frac{1}{n_2} \mathcal{L} \left[\frac{\psi_l(u)}{u} \psi_j(u) j(j+1) \mathcal{M}_{lj}^{(+)} \left\{ d_{lm} d_{jk}^* C_{lm} C_{jk} \mathcal{R}_5(l, m, j, k) \right\} \right], \quad (52)$$

$$I_{41} = n_{32} \mathcal{L} \left[\frac{\psi_l(u)}{u} \psi'_j(u) l(l+1) \mathcal{M}_{lj}^{(+)} \left\{ k c_{lm} d_{jk}^* C_{lm} C_{jk} \mathcal{R}_4(l, m, j, k) \right\} \right], \quad (53)$$

$$I_{42} = n_{32}^2 n_2 \mathcal{L} \left[\frac{\psi_l(u)}{u} \psi_j(u) l(l+1) \mathcal{M}_{lj}^{(+)} \left\{ c_{lm} c_{jk}^* C_{lm} C_{jk} \mathcal{R}_5(j, k, l, m) \right\} \right], \quad (54)$$

$$I_{51} = -n_{32} \mathcal{L} \left[\frac{\psi_l(u)}{u} \psi'_j(u) l(l+1) \mathcal{M}_{lj}^{(-)} \left\{ c_{lm} d_{jk}^* C_{lm} C_{jk} \mathcal{R}_1(j, k, l, m) \right\} \right], \quad (55)$$

$$I_{52} = -n_{32}^2 n_2 \mathcal{L} \left[\frac{\psi_l(u)}{u} \psi_j(u) l(l+1) \mathcal{M}_{lj}^{(-)} \left\{ k c_{lm} c_{jk}^* C_{lm} C_{jk} \mathcal{R}_3(l, m, j, k) \right\} \right], \quad (56)$$

$$I_{61} = n_{32} \mathcal{L} \left[\frac{\psi'_l(u)}{u} \psi_j(u) j(j+1) \mathcal{M}_{lj}^{(-)} \left\{ c_{lm} d_{jk}^* C_{lm} C_{jk} \mathcal{R}_1(l, m, j, k) \right\} \right], \quad (57)$$

$$I_{62} = -\frac{1}{n_2} \mathcal{L} \left[\frac{\psi_l(u)}{u} \psi_j(u) j(j+1) \mathcal{M}_{lj}^{(-)} \left\{ m d_{lm} d_{jk}^* C_{lm} C_{jk} \mathcal{R}_3(l, m, j, k) \right\} \right], \quad (58)$$

with

$$\mathcal{R}_1(l, m, j, k) = \int_0^\pi \sin \theta \frac{dP_l^m(\cos \theta)}{d\theta} P_j^k(\cos \theta) d\theta, \quad (59)$$

$$\mathcal{R}_2(l, m, j, k) = \int_0^\pi \sin^2 \theta \frac{dP_l^m(\cos \theta)}{d\theta} \frac{dP_j^k(\cos \theta)}{d\theta} d\theta, \quad (60)$$

$$\mathcal{R}_3(l, m, j, k) = \int_0^\pi P_l^m(\cos \theta) P_j^k(\cos \theta) d\theta, \quad (61)$$

$$\mathcal{R}_4(l, m, j, k) = \int_0^\pi \cos \theta P_l^m(\cos \theta) P_j^k(\cos \theta) d\theta, \quad (62)$$

$$\mathcal{R}_5(l, m, j, k) = \int_0^\pi \cos \theta \sin \theta \frac{dP_l^m(\cos \theta)}{d\theta} P_j^k(\cos \theta) d\theta, \quad (63)$$

and the definition

$$C_{lm} = \sqrt{\frac{(2l+1)(l-m)!}{4\pi(l+m)!}}. \quad (64)$$

Altogether, writing the non-dimensional vertical absorptive force as Q_x^{abs} , where

$$Q_x^{\text{abs}} = \frac{F_x^{\text{abs}}}{\epsilon_0 E_0^2 a^2}, \quad (65)$$

we get

$$Q_x^{\text{abs}} = -\sigma \mu_0 c \lambda \frac{n_{12} \alpha^2}{4} \Im \left[\sum_{i=1}^2 \sum_{k=1}^4 I_{ik} + \sum_{i=3}^6 \sum_{k=1}^2 I_{ik} \right]. \quad (66)$$

Note that the prefactor in the above equations, as well as the terms I_{ik} , are non-dimensional. The expression (66) is our main result.

V. RESULTS

A. Numerics

We implemented an adaptive Gauss-Kronrod rule to calculate the integrals in Eqs. (22) – (24) and (43) – (58). By employing the symmetry properties of the integrals over the Legendre polynomials (Eqs. (59) – (63)), we were able to greatly reduce the number of integrals to be computed. To make sure that the sum over l and j in Eq. (39) converged properly for our chosen cut-off value, we plotted the total absorptive force on the sphere versus increasing cut-off, l_{max} , in l (we used the same cut-off for l and j). In Fig. 2, we give an example for p polarization using several values of α . The total force is normalized to the $l_{\text{max}} = 30$ result; all other parameters are given in the figure caption. This figure clearly suggests that, for a given value of α , there is a narrow range in l which accounts for most of the absorptive force. Moreover, it is seen that this range of important l -values moves to higher l and broadens with increasing α . In the inset, we

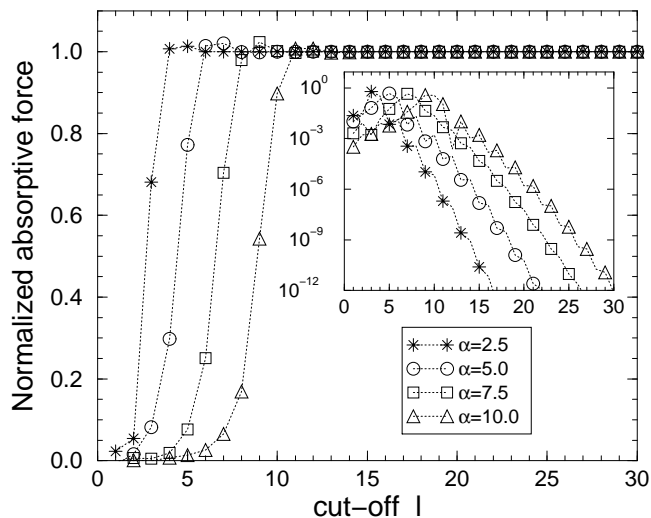


FIG. 2: Plot of the total absorptive force versus increasing cut-off in Eq. (39) for 4 values of α : 2.5, 5.0, 7.5, and 10.0, with $n_1 = 1.75$, $n_2 = 1.33$, and $n_3 = 1.50$. The inset shows the absolute value of the difference in the total force using l and $(l - 1)$ respectively, as cut-offs.

plot on a linear-log scale the absolute value of the difference in the total force using l and $(l - 1)$ respectively, as cut-offs. The inset indicates that contributions to the absorptive force from large l -values (large with respect to the l -value of the peak) are exponentially suppressed. Hence, for the range of values for α , n_1 , n_2 , and n_3 studied in this article, we need only consider contributions to the force from $l \leq 30$.

It is of interest to point out that the main features of Fig. 2 can be understood from a physical point of view. (This kind of argument is frequently made use of in connection with Casimir-related calculations; cf. for instance, Ref. [19]). The most significant angular momenta are those that are of the same order of magnitude as, or are somewhat smaller than, the angular momentum corresponding to grazing incidence on the sphere. Consider now a photon with energy $\hbar\omega$ and momentum $\hbar k_2$ that just touches the surface of the sphere. Its angular momentum is $\hbar k_2 a$. Setting the angular momentum equal to $\hbar l$, we thus obtain $l = k_2 a = \alpha$. Thus, the most significant values of l should be expected to be $l \lesssim \alpha$. This is seen to be in accordance with the calculated results in Fig. 2. In view of the crudeness of the argument, the agreement is actually better than we had reason to expect.

B. Discussion of the figures

Illustrative examples of the behavior of the non-dimensional vertical absorptive force are shown in Figs. 3 – 5. The angle of incidence is $\theta_1 = 51^\circ$ everywhere. In the case of p polarization, $E_0 = E_{\parallel}^{(1)}$, whereas for s

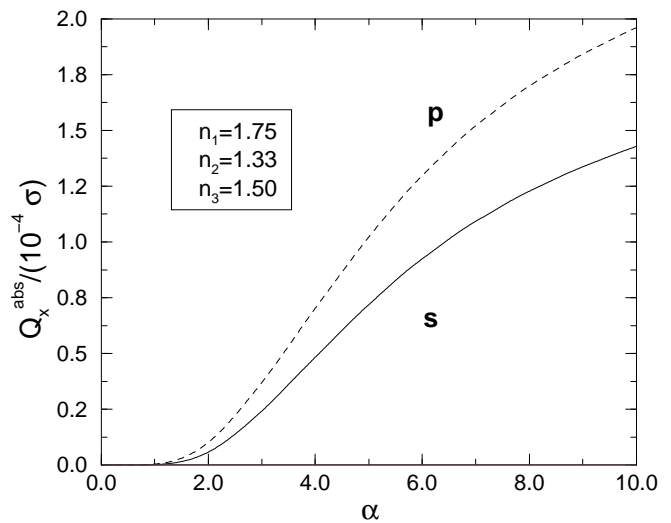


FIG. 3: Non-dimensional vertical absorptive force $Q_x^{\text{abs}} = F_x^{\text{abs}} / (\epsilon_0 E_0^2 a^2)$ versus particle size parameter $\alpha = k_2 a$ for the set of refractive indices shown. The two states of polarization for the incident beam are distinguished. Here, as well as in the subsequent figures, $\theta_1 = 51^\circ$. Also, all figures refer to sphere resting on the plate, *i.e.* to $h = a$. The figure is scaled against the conductivity σ of the sphere.

polarization, $E_0 = E_{\perp}^{(1)}$. When the incident field is taken to be a plane wave, the amplitudes $E_{\parallel}^{(1)}$ and $E_{\perp}^{(1)}$ are constants. It is to be kept in mind that, in order to lift the sphere from the plate, the positive absorptive force has to overcome not only gravity, but also the negative surface force F_x^{surf} that was calculated in Ref. [2] for the same values of $\{n_1, n_2, n_3\}$ as we consider here. The cases treated in the two papers are thus directly comparable.

Similarly to Ref. [2], all curves in Figs. 3 – 5 refer to the case of contact between sphere and plate, *i.e.* to $h = a$. From Eqs. (19) and (20), it is seen that A_{lm} and B_{lm} contain $\exp(-\beta h)$ as a common factor. The same property is carried over to the coefficients c_{lm} and d_{lm} , according to Eqs. (A.21) and (A.22). As the absorptive force is quadratic in the last-mentioned coefficients, it follows that Q_x^{abs} at an arbitrary height h is equal to $\exp[-2\beta(h - a)]$ times the value that can be read off from Figs. 3 – 5. No figures need to be worked out to show the dependence of the force with height above the plate.

In order to interpret the figures physically, it is helpful to consider a concrete example. Let us relate our discussion essentially to the situation considered in Section 3: incident plane wave of power $P = 150$ mW, corresponding to $\epsilon_0 E_0^2 a^2 = 0.13$ pN when the radius of the sphere is $a = 1 \mu\text{m}$. If the density of the sphere is 2.4 g/cm^3 (the same density as for glass), the weight of it is $mg = 0.10$ pN. Moreover, $n_3 = 1.50$, $n_2 = 1.33$ (water), whereas the size parameter is $\alpha = 7.9$ for Nd:YAG laser light. Let us look for the necessary value of σ in order to satisfy the condition for elevation of the sphere, just above the plate. The condition is $F_x^{\text{abs}} = mg + |F_x^{\text{surf}}|$. Expressed

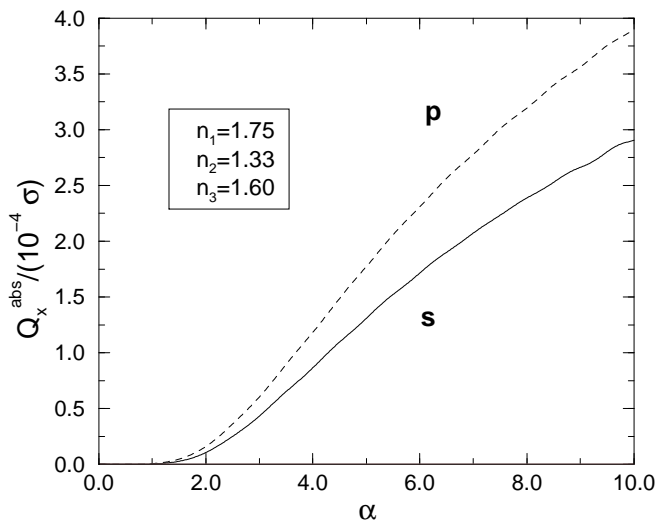


FIG. 4: Same as for Fig. 3, but with a higher (dominant real part of) refractive index ($n_3 = 1.60$) in the sphere.

non-dimensionally,

$$Q_x^{\text{abs}} = \frac{mg}{\epsilon_0 E_0^2 a^2} + |Q_x^{\text{surf}}|. \quad (67)$$

From Fig. 3 we read off, when choosing for definiteness the case of p polarization, $Q_x^{\text{abs}}/(10^{-4}\sigma) = 1.7$, whereas from Fig. 4 in [2] we read off $Q_x^{\text{surf}} = -0.35$ for the same value of α . This leads to a relatively high value of σ , about 6600 S/m ($S \equiv \Omega^{-1}$). In our example, the influence of the weight of the sphere is relatively large because the incident power is so moderate. If we increase P to 1 watt, we get $\epsilon_0 E_0^2 a^2 = 0.87$ pN, resulting in a somewhat lower value, $\sigma \approx 2700$ S/m.

For glass, at optical wavelengths, the effective conductivity σ is very small. (The static conductivity is extremely small, $\sigma_{\text{stat}} \sim 10^{-12}$ S/m.) Even for higher wavelengths such as $\lambda_0 = 8.0 \mu\text{m}$, the value $\sigma = 550$ S/m given in Eq. (6) is insufficient to account for the lifting force. For water, at optical wavelengths, as we have seen in Eq. (5), the effective conductivity is even smaller. We can thus immediately conclude that absorption is *not* the physical reason for the elevation of the sphere in the Kawata-Sugiura experiment. It is likely that there were surfactants on the spheres in this experiment, and hence, that a theoretical description of the kind given in Ref. [4] is most appropriate in this case. For other materials where the conductivities are higher, for instance for carbon ($\sigma_{\text{stat}} = 0.77 \times 10^5$ S/m), the absorption-generated elevation of microspheres should be quite possible physically. One must however be aware of the algebraic restriction made in the present paper to simplify calculations: our calculation relied on the property that $\sigma/\epsilon_0\omega \ll 1$ (cf. Eq. (2)). This restriction made it possible to take the refractive index n_3 to be real, inside the integrals in Section 4. Since $\epsilon_0\omega \approx 10^5$ S/m, we can no longer expect high accuracy from the formalism when $\sigma \gg 10^4$ S/m,

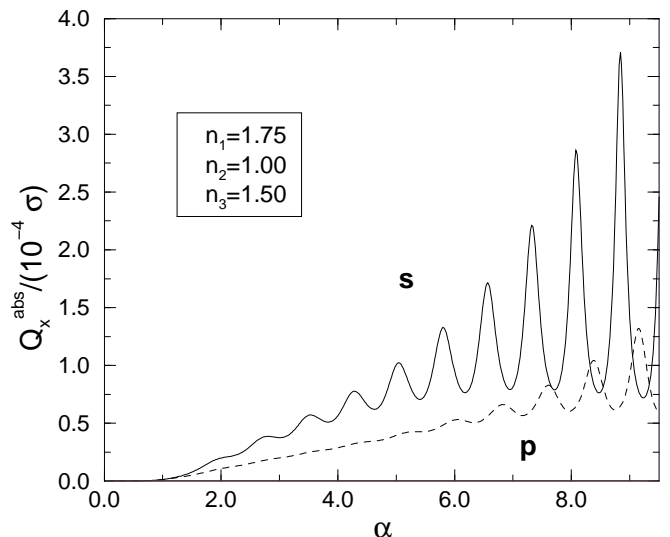


FIG. 5: Same as for Fig. 3, but with vacuum ($n_2 = 1$) surrounding the sphere.

at optical frequencies.

Consider finally the remaining figures: Fig. 4 shows that when the refractive index in the sphere increases from 1.50 to 1.60, the absorptive force increases. This is as we would expect. Moreover, if the difference between interior and exterior indices increases, the Riccati-Bessel functions cause the force to become more oscillatory in character. The changes are clearly shown, if we compare Fig. 3 with Fig. 5. Increasing differences between the refractive indices effectively mean enhancing the geometrical-optics properties of the system. There is also a dependence of the force upon the two different polarization states of the beam. No simple physical explanation of this dependence seems to exist.

VI. CONCLUSIONS

We can summarize as follows:

1. The strategy of the above calculation has been to identify the evanescent field with the incident field on the sphere. The theory makes use of wave optics, and is thus applicable even when the wavelength is of the same magnitude as the sphere diameter.
2. The main novel development of the present paper in comparison with Ref. [2] is the calculation in Section 4 of the vertical absorptive force, assuming the refractive index \bar{n}_3 in the sphere to be complex. The calculation rests upon the approximation that $\sigma/\epsilon_0\omega \ll 1$, so that the fields inside the sphere can be evaluated as if the material were a perfect dielectric. The surface force is thus calculated from Eq. (26) assuming $\bar{n}_3 = n_3$ to be real. The absorptive force is calculated from Eq. (30).
3. The results of Figs. 3 – 5 show that in order to account for elevation of the micrometer-sphere, the con-

ductivity σ must be at least as large as about 10^3 S/m. This applies, for instance, to media like carbon.

4. For latex or glass spheres, used in the Kawata-Sugiura experiment [1], the absorptive force seems to be too weak to account for the elevation force. Most probably, the observed elevation force was due largely to impurities or a film on the surface of the sphere, making it partly conducting. Cf. also Ref. [4]. The absorption is sensitive with respect to impurities, and it is at present difficult to estimate to which degree the absorption is important in practice.

5. As a final general remark: the subject of radiation pressure on particles in the evanescent field is a many-faceted phenomenon which is not yet fully understood, and it is a very active subject. In addition to the references given above, the reader is referred also to recent papers in which the dipole method is made use of, in order to calculate the force of an evanescent wave over dielectric and metallic surfaces [20, 21].

VII. ACKNOWLEDGEMENTS

E.A. was supported by NSF through grants DMR97-31511 and DMR01-04987. Computational support

was provided by the Ohio Supercomputer Center and the Norwegian University of Science and Technology (NTNU).

APPENDIX A: EXPANSIONS OF THE ELECTROMAGNETIC FIELDS

For convenience, we summarize the expansions for the incident, (*i*), the scattered, (*s*), and the internal, (*w*), field components. As mentioned in the main text, subscript 1 refers to the non-absorbing substrate, subscript 2 to the non-absorbing medium around the sphere (refractive index n_2), and subscript 3 to the absorbing sphere whose complex refractive index is \bar{n}_3 . The relative refractive index is $\bar{n}_{32} = \bar{n}_3/n_2$. Furthermore, E_0 and H_0 refer to the incoming plane wave in the substrate, the non-dimensional wave number and distance is $\alpha = k_2 a = n_2 \omega a/c$, and $\tilde{r} = r/a$ respectively.

The formulas below are general. As mentioned in the main text, in the practical calculations of the coefficients A_{lm} and B_{lm} we took however the refractive index \bar{n}_3 to be real.

Incident field

$$E_r^{(i)} = \frac{E_0}{\tilde{r}^2} \sum_{l=1}^{\infty} \sum_{m=-l}^l l(l+1) A_{lm} \psi_l(\alpha \tilde{r}) Y_{lm}, \quad (\text{A.1})$$

$$E_{\theta}^{(i)} = \frac{\alpha E_0}{\tilde{r}} \sum_{l=1}^{\infty} \sum_{m=-l}^l \left[A_{lm} \psi_l'(\alpha \tilde{r}) \frac{\partial Y_{lm}}{\partial \theta} - \frac{m}{n_2} B_{lm} \psi_l(\alpha \tilde{r}) \frac{Y_{lm}}{\sin \theta} \right], \quad (\text{A.2})$$

$$E_{\varphi}^{(i)} = \frac{\alpha E_0}{\tilde{r}} \sum_{l=1}^{\infty} \sum_{m=-l}^l \left[i m A_{lm} \psi_l'(\alpha \tilde{r}) \frac{Y_{lm}}{\sin \theta} - \frac{i}{n_2} B_{lm} \psi_l(\alpha \tilde{r}) \frac{\partial Y_{lm}}{\partial \theta} \right], \quad (\text{A.3})$$

$$H_r^{(i)} = \frac{H_0}{\tilde{r}^2} \sum_{l=1}^{\infty} \sum_{m=-l}^l l(l+1) B_{lm} \psi_l(\alpha \tilde{r}) Y_{lm}, \quad (\text{A.4})$$

$$H_{\theta}^{(i)} = \frac{\alpha H_0}{\tilde{r}} \sum_{l=1}^{\infty} \sum_{m=-l}^l \left[B_{lm} \psi_l'(\alpha \tilde{r}) \frac{\partial Y_{lm}}{\partial \theta} + m n_2 A_{lm} \psi_l(\alpha \tilde{r}) \frac{Y_{lm}}{\sin \theta} \right], \quad (\text{A.5})$$

$$H_{\varphi}^{(i)} = \frac{\alpha H_0}{\tilde{r}} \sum_{l=1}^{\infty} \sum_{m=-l}^l \left[i m B_{lm} \psi_l'(\alpha \tilde{r}) \frac{Y_{lm}}{\sin \theta} + i n_2 A_{lm} \psi_l(\alpha \tilde{r}) \frac{\partial Y_{lm}}{\partial \theta} \right]. \quad (\text{A.6})$$

Scattered field

$$E_r^{(s)} = \frac{E_0}{\tilde{r}^2} \sum_{l=1}^{\infty} \sum_{m=-l}^l l(l+1) a_{lm} \xi_l^{(1)}(\alpha \tilde{r}) Y_{lm}, \quad (\text{A.7})$$

$$E_{\theta}^{(s)} = \frac{\alpha E_0}{\tilde{r}} \sum_{l=1}^{\infty} \sum_{m=-l}^l \left[a_{lm} \xi_l^{(1)'}(\alpha \tilde{r}) \frac{\partial Y_{lm}}{\partial \theta} - \frac{m}{n_2} b_{lm} \xi_l^{(1)}(\alpha \tilde{r}) \frac{Y_{lm}}{\sin \theta} \right], \quad (\text{A.8})$$

$$E_\varphi^{(s)} = \frac{\alpha E_0}{\tilde{r}} \sum_{l=1}^{\infty} \sum_{m=-l}^l \left[i m a_{lm} \xi_l^{(1)'}(\alpha \tilde{r}) \frac{Y_{lm}}{\sin \theta} - \frac{i}{n_2} b_{lm} \xi_l^{(1)}(\alpha \tilde{r}) \frac{\partial Y_{lm}}{\partial \theta} \right], \quad (\text{A.9})$$

$$H_r^{(s)} = \frac{H_0}{\tilde{r}^2} \sum_{l=1}^{\infty} \sum_{m=-l}^l l(l+1) b_{lm} \xi_l^{(1)}(\alpha \tilde{r}) Y_{lm}, \quad (\text{A.10})$$

$$H_\theta^{(s)} = \frac{\alpha H_0}{\tilde{r}} \sum_{l=1}^{\infty} \sum_{m=-l}^l \left[b_{lm} \xi_l^{(1)'}(\alpha \tilde{r}) \frac{\partial Y_{lm}}{\partial \theta} + m n_2 a_{lm} \xi_l^{(1)}(\alpha \tilde{r}) \frac{Y_{lm}}{\sin \theta} \right], \quad (\text{A.11})$$

$$H_\varphi^{(s)} = \frac{\alpha H_0}{\tilde{r}} \sum_{l=1}^{\infty} \sum_{m=-l}^l \left[i m b_{lm} \xi_l^{(1)'}(\alpha \tilde{r}) \frac{Y_{lm}}{\sin \theta} + i n_2 a_{lm} \xi_l^{(1)}(\alpha \tilde{r}) \frac{\partial Y_{lm}}{\partial \theta} \right]. \quad (\text{A.12})$$

Internal field

$$E_r^{(w)} = \frac{E_0}{\tilde{r}^2} \sum_{l=1}^{\infty} \sum_{m=-l}^l l(l+1) c_{lm} \psi_l(\bar{n}_{32} \alpha \tilde{r}) Y_{lm}, \quad (\text{A.13})$$

$$E_\theta^{(w)} = \frac{\alpha E_0}{\tilde{r}} \sum_{l=1}^{\infty} \sum_{m=-l}^l \left[\bar{n}_{32} c_{lm} \psi_l'(\bar{n}_{32} \alpha \tilde{r}) \frac{\partial Y_{lm}}{\partial \theta} - \frac{m}{n_2} d_{lm} \psi_l(\bar{n}_{32} \alpha \tilde{r}) \frac{Y_{lm}}{\sin \theta} \right], \quad (\text{A.14})$$

$$E_\varphi^{(w)} = \frac{\alpha E_0}{\tilde{r}} \sum_{l=1}^{\infty} \sum_{m=-l}^l \left[i m \bar{n}_{32} c_{lm} \psi_l'(\bar{n}_{32} \alpha \tilde{r}) \frac{Y_{lm}}{\sin \theta} - \frac{i}{n_2} d_{lm} \psi_l(\bar{n}_{32} \alpha \tilde{r}) \frac{\partial Y_{lm}}{\partial \theta} \right], \quad (\text{A.15})$$

$$H_r^{(w)} = \frac{H_0}{\tilde{r}^2} \sum_{l=1}^{\infty} \sum_{m=-l}^l l(l+1) d_{lm} \psi_l(\bar{n}_{32} \alpha \tilde{r}) Y_{lm}, \quad (\text{A.16})$$

$$H_\theta^{(w)} = \frac{\alpha H_0}{\tilde{r}} \sum_{l=1}^{\infty} \sum_{m=-l}^l \left[\bar{n}_{32} d_{lm} \psi_l'(\bar{n}_{32} \alpha \tilde{r}) \frac{\partial Y_{lm}}{\partial \theta} + m n_2 \bar{n}_{32}^2 c_{lm} \psi_l(\bar{n}_{32} \alpha \tilde{r}) \frac{Y_{lm}}{\sin \theta} \right], \quad (\text{A.17})$$

$$H_\varphi^{(w)} = \frac{\alpha H_0}{\tilde{r}} \sum_{l=1}^{\infty} \sum_{m=-l}^l \left[i m \bar{n}_{32} d_{lm} \psi_l'(\bar{n}_{32} \alpha \tilde{r}) \frac{Y_{lm}}{\sin \theta} + i n_2 \bar{n}_{32}^2 c_{lm} \psi_l(\bar{n}_{32} \alpha \tilde{r}) \frac{\partial Y_{lm}}{\partial \theta} \right]. \quad (\text{A.18})$$

Everywhere, primes denote differentiation with respect to the whole argument.

Relations between coefficients

$$a_{lm} = \frac{\psi_l'(\bar{n}_{32} \alpha) \psi_l(\alpha) - \bar{n}_{32} \psi_l(\bar{n}_{32} \alpha) \psi_l'(\alpha)}{\bar{n}_{32} \psi_l(\bar{n}_{32} \alpha) \xi_l^{(1)'}(\alpha) - \psi_l'(\bar{n}_{32} \alpha) \xi_l^{(1)}(\alpha)} A_{lm}, \quad (\text{A.19})$$

$$b_{lm} = \frac{\bar{n}_{32} \psi_l'(\bar{n}_{32} \alpha) \psi_l(\alpha) - \psi_l(\bar{n}_{32} \alpha) \psi_l'(\alpha)}{\psi_l(\bar{n}_{32} \alpha) \xi_l^{(1)'}(\alpha) - \bar{n}_{32} \psi_l'(\bar{n}_{32} \alpha) \xi_l^{(1)}(\alpha)} B_{lm}, \quad (\text{A.20})$$

$$c_{lm} = \frac{i}{\bar{n}_{32}^2 \psi_l(\bar{n}_{32} \alpha) \xi_l^{(1)'}(\alpha) - \bar{n}_{32} \psi_l'(\bar{n}_{32} \alpha) \xi_l^{(1)}(\alpha)} A_{lm}, \quad (\text{A.21})$$

$$d_{lm} = \frac{i}{\psi_l(\bar{n}_{32} \alpha) \xi_l^{(1)'}(\alpha) - \bar{n}_{32} \psi_l'(\bar{n}_{32} \alpha) \xi_l^{(1)}(\alpha)} B_{lm}. \quad (\text{A.22})$$

Here the Wronskian is $W\{\psi_l, \xi_l^{(1)}\} = i$.

APPENDIX B: TABLE OF A_{lm} AND B_{lm}

We include a table of the numerical values for the real and imaginary parts of A_{lm} and B_{lm} for an evanescent field. The coefficients are calculated for p polarization, and we have set $a = 1$ and $e^{-\beta h} = 1$ in Eqs. (19) and (20). For space considerations, we only give the coefficients up to $l = 7$.

l	m	$\Re\{A_{lm}\}$	$\Im\{A_{lm}\}$	$\Re\{B_{lm}\}$	$\Im\{B_{lm}\}$	l	m	$\Re\{A_{lm}\}$	$\Im\{A_{lm}\}$	$\Re\{B_{lm}\}$	$\Im\{B_{lm}\}$
1	-1	7.8951e-14	-3.5261e-14	4.5863e-14	1.0269e-13	5	2	1.1689e-14	2.6172e-14	3.1349e-14	-1.4001e-14
1	0	-1.0417e-14	-2.3324e-14	0.0	0.0	5	3	6.2653e-15	-2.7982e-15	-3.5248e-15	-7.8921e-15
1	1	-7.8951e-14	3.5261e-14	4.5863e-14	1.0269e-13	5	4	-4.0248e-16	-9.0116e-16	-1.1595e-15	5.1784e-16
2	-2	-1.2570e-14	5.6142e-15	-7.3021e-15	-1.6350e-14	5	5	-7.3610e-17	3.2876e-17	4.2760e-17	9.5741e-17
2	-1	2.8048e-14	6.2800e-14	-7.8266e-14	3.4955e-14	6	-6	-1.4028e-17	6.2652e-18	-8.1489e-18	-1.8246e-17
2	0	3.0791e-14	-1.3752e-14	0.0	0.0	6	-5	8.7334e-17	1.9554e-16	-2.5213e-16	1.1261e-16
2	1	-2.8048e-14	-6.2800e-14	-7.8266e-14	3.4955e-14	6	-4	1.6276e-15	-7.2694e-16	9.2343e-16	2.0676e-15
2	2	-1.2570e-14	5.6142e-15	7.3021e-15	1.6350e-14	6	-3	-3.9706e-15	-8.8903e-15	1.0972e-14	-4.9002e-15
3	-3	2.1752e-15	-9.7150e-16	1.2636e-15	2.8292e-15	6	-2	-3.1171e-14	1.3922e-14	-1.6060e-14	-3.5958e-14
3	-2	-7.7601e-15	-1.7375e-14	2.2116e-14	-9.8777e-15	6	-1	2.8039e-14	6.2781e-14	-5.7903e-14	2.5861e-14
3	-1	-5.7659e-14	2.5752e-14	-3.0232e-14	-6.7690e-14	6	0	6.0270e-14	-2.6918e-14	0.0	0.0
3	0	1.6820e-14	3.7661e-14	0.0	0.0	6	1	-2.8039e-14	-6.2781e-14	-5.7903e-14	2.5861e-14
3	1	5.7659e-14	-2.5752e-14	-3.0232e-14	-6.7690e-14	6	2	-3.1171e-14	1.3922e-14	1.6060e-14	3.5958e-14
3	2	-7.7601e-15	-1.7375e-14	-2.2116e-14	9.8777e-15	6	3	3.9706e-15	8.8903e-15	1.0972e-14	-4.9002e-15
3	3	-2.1752e-15	9.7150e-16	1.2636e-15	2.8292e-15	6	4	1.6276e-15	-7.2694e-16	-9.2343e-16	-2.0676e-15
4	-4	-3.9427e-16	1.7609e-16	-2.2903e-16	-5.1281e-16	6	5	-8.7334e-17	-1.9554e-16	-2.5213e-16	1.1261e-16
4	-3	1.8142e-15	4.0620e-15	-5.2075e-15	2.3258e-15	6	6	-1.4028e-17	6.2652e-18	8.1489e-18	1.8246e-17
4	-2	2.1681e-14	-9.6834e-15	1.1989e-14	2.6843e-14	7	-7	2.7140e-18	-1.2121e-18	1.5766e-18	3.5300e-18
4	-1	-2.5411e-14	-5.6895e-14	6.2106e-14	-2.7738e-14	7	-6	-1.8745e-17	-4.1970e-17	5.4194e-17	-2.4204e-17
4	0	-4.4609e-14	1.9923e-14	0.0	0.0	7	-5	-3.9999e-16	1.7865e-16	-2.2806e-16	-5.1063e-16
4	1	2.5411e-14	5.6895e-14	6.2106e-14	-2.7738e-14	7	-4	1.1736e-15	2.6278e-15	-3.2899e-15	1.4693e-15
4	2	2.1681e-14	-9.6834e-15	-1.1989e-14	-2.6843e-14	7	-3	1.2042e-14	-5.3781e-15	6.4860e-15	1.4522e-14
4	3	-1.8142e-15	-4.0620e-15	-5.2075e-15	2.3258e-15	7	-2	-1.6489e-14	-3.6919e-14	4.0869e-14	-1.8253e-14
4	4	-3.9427e-16	1.7609e-16	2.2903e-16	5.1281e-16	7	-1	-6.8637e-14	3.0655e-14	-2.5861e-14	-5.7905e-14
5	-5	7.3610e-17	-3.2876e-17	4.2760e-17	9.5741e-17	7	0	3.1083e-14	6.9595e-14	0.0	0.0
5	-4	-4.0248e-16	-9.0116e-16	1.1595e-15	-5.1784e-16	7	1	6.8637e-14	-3.0655e-14	-2.5861e-14	-5.7905e-14
5	-3	-6.2653e-15	2.7982e-15	-3.5248e-15	-7.8921e-15	7	2	-1.6489e-14	-3.6919e-14	-4.0869e-14	1.8253e-14
5	-2	1.1689e-14	2.6172e-14	-3.1349e-14	1.4001e-14	7	3	-1.2042e-14	5.3781e-15	6.4860e-15	1.4522e-14
5	-1	5.8803e-14	-2.6263e-14	2.6420e-14	5.9156e-14	7	4	1.1736e-15	2.6278e-15	3.2899e-15	-1.4693e-15
5	0	-2.3242e-14	-5.2039e-14	0.0	0.0	7	5	3.9999e-16	-1.7865e-16	-2.2806e-16	-5.1063e-16
5	1	-5.8803e-14	2.6263e-14	2.6420e-14	5.9156e-14	7	6	-1.8745e-17	-4.1970e-17	-5.4194e-17	2.4204e-17
						7	7	-2.7140e-18	1.2121e-18	1.5766e-18	3.5300e-18

-
- [1] S. Kawata and T. Sugiura, "Movement of micrometer-sized particles in the evanescent field of a laser beam", *Opt. Lett.* **17**, 772-774 (1992).
- [2] E. Almaas and I. Brevik, "Radiation forces on a micrometer-sized sphere in an evanescent field", *J. Opt. Soc. Am. B* **12**, 2429-2438 (1995).
- [3] M. Vilfan, I. Muševič, and M. Čopič, *Europhys. Lett.* **43**, 41-46 (1998).
- [4] M. Lester and M. Nieto-Vesperinas, "Optical forces on microparticles in an evanescent laser field", *Opt. Lett.* **24**, 936-938 (1999).
- [5] V. G. Levich, *Physicochemical Hydrodynamics* (Prentice-Hall, N.J., 1962).
- [6] L. D. Landau and E. M. Lifshitz, *Fluid Mechanics*, 2nd ed. (Pergamon Press, Oxford, 1987), Sect. 63.
- [7] J. D. Jackson, *Classical Electrodynamics*, 3rd ed. (John Wiley & Sons, New York, 1999).
- [8] J. P. Barton, D. R. Alexander, and S. A. Schaub, "Internal and near-surface electromagnetic fields for a spherical particle irradiated by a focused laser beam", *J. Appl. Phys.* **64**, 1632-1639 (1988).
- [9] J. A. Stratton, *Electromagnetic Theory* (McGraw-Hill, New York, 1941).
- [10] H. R. Philipp, in *Handbook of Optical Constants of Solids*, edited by E. D. Palik (Academic Press, Orlando, Florida, 1985), p. 749.
- [11] J. P. Barton, D. R. Alexander, and S. A. Schaub, "Theoretical determination of net radiation force and torque for a spherical particle illuminated by a focused laser beam", *J. Appl. Phys.* **66**, 4594-4602 (1989).
- [12] Ø. Farsund and B. U. Felderhof, "Force, torque, and absorbed energy for a body of arbitrary shape and constitution in an electromagnetic radiation field", *Physica A* **227**, 108-130 (1996).
- [13] M. Kerker, *The Scattering of Light* (Academic, New York, 1969).
- [14] M. Born and E. Wolf, *Principles of Optics*, 6th ed. (Pergamon, Oxford, 1991).
- [15] I. Brevik, "Experiments in phenomenological electrodynamics and the electromagnetic energy-momentum tensor", *Phys. Rep.* **52**, 133-201 (1979).
- [16] P. C. Chaumet and M. Nieto-Vesperinas, "Time-averaged

- total force on a dipolar sphere in an electromagnetic field", *Opt. Lett.* **25**, 1065-1067 (2000).
- [17] A. Ashkin, J. M. Dziedzic, J. E. Bjorkholm, and S. Chu, "Observation of a single-beam gradient force optical trap for dielectric particles", *Opt. Lett.* **11**, 288-290 (1986).
- [18] L. D. Landau and E. M. Lifshitz, *Electrodynamics of Continuous Media*, 2nd ed. (Pergamon, Oxford, 1984), Sect. 93.
- [19] I. Brevik and V. N. Marachevsky, "Casimir surface force on a dilute dielectric ball", *Phys. Rev. D* **60**, 085006 (12 pages) (1999).
- [20] P. C. Chaumet and M. Nieto-Vesperinas, "Coupled dipole method determination of the electromagnetic force on a particle over a flat dielectric substrate", *Phys. Rev. B* **61**, 14119-14127 (2000).
- [21] P. C. Chaumet and M. Nieto-Vesperinas, "Electromagnetic force on a metallic particle in the presence of a dielectric surface", *Phys. Rev. B* **62**, 11185-11191 (2000).